

## 6.3: Electronic Structure of Complexes (Part 2)

### Molecular orbital theory of transition metal complexes

The characteristics of transition metal-ligand bonds become clear by an analysis of the molecular orbitals of a 3d metal coordinated by six identical ligands in octahedral complexes  $[ML_6]$ . As the result of the interaction between the metal d and ligand orbitals, bonding, non-bonding and anti-bonding complex molecular orbitals are formed.

Generally, the energy levels of the ligand orbitals are lower than those of the metal orbitals, bonding orbitals have more ligand character and non-bonding and anti-bonding orbitals have more metal character. The processes of formation of the  $\sigma$  and  $\pi$  molecular orbitals are described step by step below.

#### $\sigma$ bond

Firstly, consider the M-L  $\sigma$  bond among interactions of the metal s, p, d and ligand orbitals by assuming the position of a metal at the origin of the Cartesian coordinate system and locating ligands on the coordinate axes. As the  $\sigma$  bond is a nodeless bond along the bonding axes, the metal s orbital ( $a_{1g}$ , non-degenerate),  $p_x$ ,  $p_y$ ,  $p_z$  orbitals ( $t_{1u}$ , triply-degenerate), and  $d_{x^2-y^2}$ ,  $d_{z^2}$  orbitals ( $e_g$ , doubly-degenerate) fit symmetry (+, - signs) and orbital shapes with the ligands'  $\sigma$  orbitals (Figure 6.3.9).

When the ligand orbitals are  $\sigma_1$  and  $\sigma_2$  along the x-axis,  $\sigma_3$  and  $\sigma_4$  along the y-axis, and  $\sigma_5$  and  $\sigma_6$  along the z-axis in Figure 6.3.5, six ligand atomic orbitals are grouped by making linear combinations according to the symmetry of the metal orbitals. Then the orbital to fit with the metal  $a_{1g}$  orbital is  $a_{1g}$  ( $\sigma_1 + \sigma_2 + \sigma_3 + \sigma_4 + \sigma_5 + \sigma_6$ ), the one to fit with the metal  $t_{1u}$  orbitals is  $t_{1u}$  ( $\sigma_1 - \sigma_2, \sigma_3 - \sigma_4, \sigma_5 - \sigma_6$ ) and the one to fit with the metal  $e_g$  orbitals is  $e_g$  ( $\sigma_1 + \sigma_2 - \sigma_3 - \sigma_4, \sigma_5 + \sigma_6 - \sigma_1 - \sigma_2 - \sigma_3 - \sigma_4$ ). There is a bonding interaction between the metal  $e_g$  orbitals and the ligand group orbitals and bonding and anti-bonding molecular orbitals are formed. The relation is shown in Figure 6.3.10.

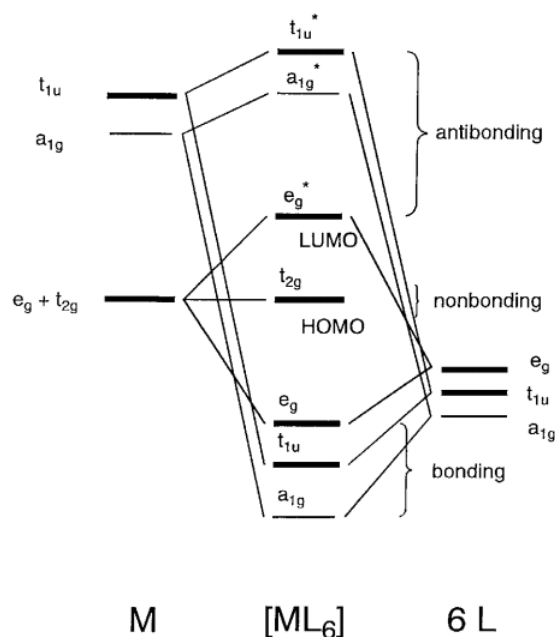


Figure 6.3.10: - Bonding and anti-bonding M(metal)-L(ligand) molecular orbitals.

The levels of the molecular orbitals from the lowest energy are bonding ( $a_{1g} < t_{1u} < e_g$ ) < non-bonding ( $t_{2g}$ ) < anti-bonding ( $e_g^* < a_{1g}^* < t_{1u}^*$ ). For example, in a complex like  $[Co(NH_3)_6]^{3+}$ , 18 valence electrons, 6 from cobalt and 12 from ammonia, occupy 9 orbitals from the bottom up, and  $t_{2g}$  is the HOMO and  $e_g^*$  the LUMO. The energy difference between the two levels corresponds to the ligand field splitting. Namely, the  $e_g$  set ( $d_{x^2-y^2}$ ,  $d_{z^2}$ ) and the ligands on the corner of the octahedron form the bonding  $\sigma$  orbitals but the  $t_{2g}$  set ( $d_{xy}$ ,  $d_{yz}$ ,  $d_{xz}$ ) remain non-bonding because the orbitals are not directed to the ligand  $\sigma$  orbitals.

#### $\pi$ bond

When the ligand atomic orbitals have  $\pi$  symmetry (i.e. with nodes) through the bond axis, the  $e_g$  orbitals ( $d_{x^2-y^2}$ ) are non-bonding and the  $t_{2g}$  orbitals ( $d_{xy}$ ,  $d_{yz}$ ,  $d_{xz}$ ) have bonding interactions with them (Figure 6.3.11). In halide ions,  $X^-$ , or aqua ligands,  $H_2O$ , the

$\pi$  symmetrical p orbitals have lower energy than the metal  $t_{2g}$  orbitals and a bonding molecular orbital, which is lower than the  $t_{2g}$  orbital, and an anti-bonding molecular orbital, which is higher than the  $t_{2g}$  orbitals, form. Consequently, the energy difference  $\Delta_o$  between  $e_g$  and the anti-bonding orbitals becomes smaller. On the other hand, for the ligands having anti-bonding  $\pi$  orbitals within the molecule, such as carbon monoxide or ethylene, the  $\pi^*$  orbitals match the shape and symmetry of the  $t_{2g}$  orbitals and the molecular orbitals shown in Fig 6.12 (b) form. As a result, the energy level of the bonding orbitals decreases and  $\Delta_o$  becomes larger.

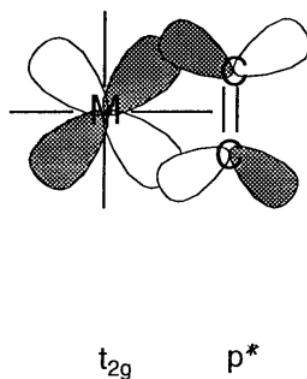
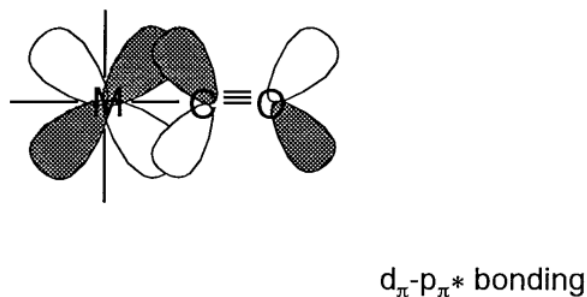
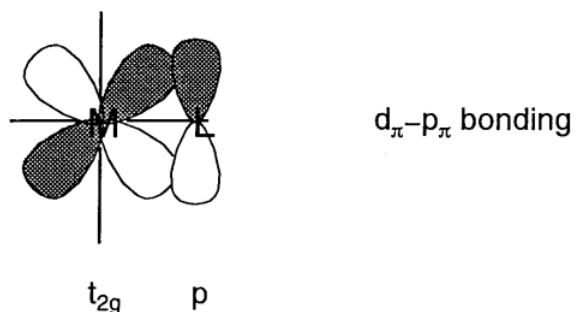


Figure 6.3.11: - The relation between the metal and ligand orbitals in formation of a  $\pi$  bond.

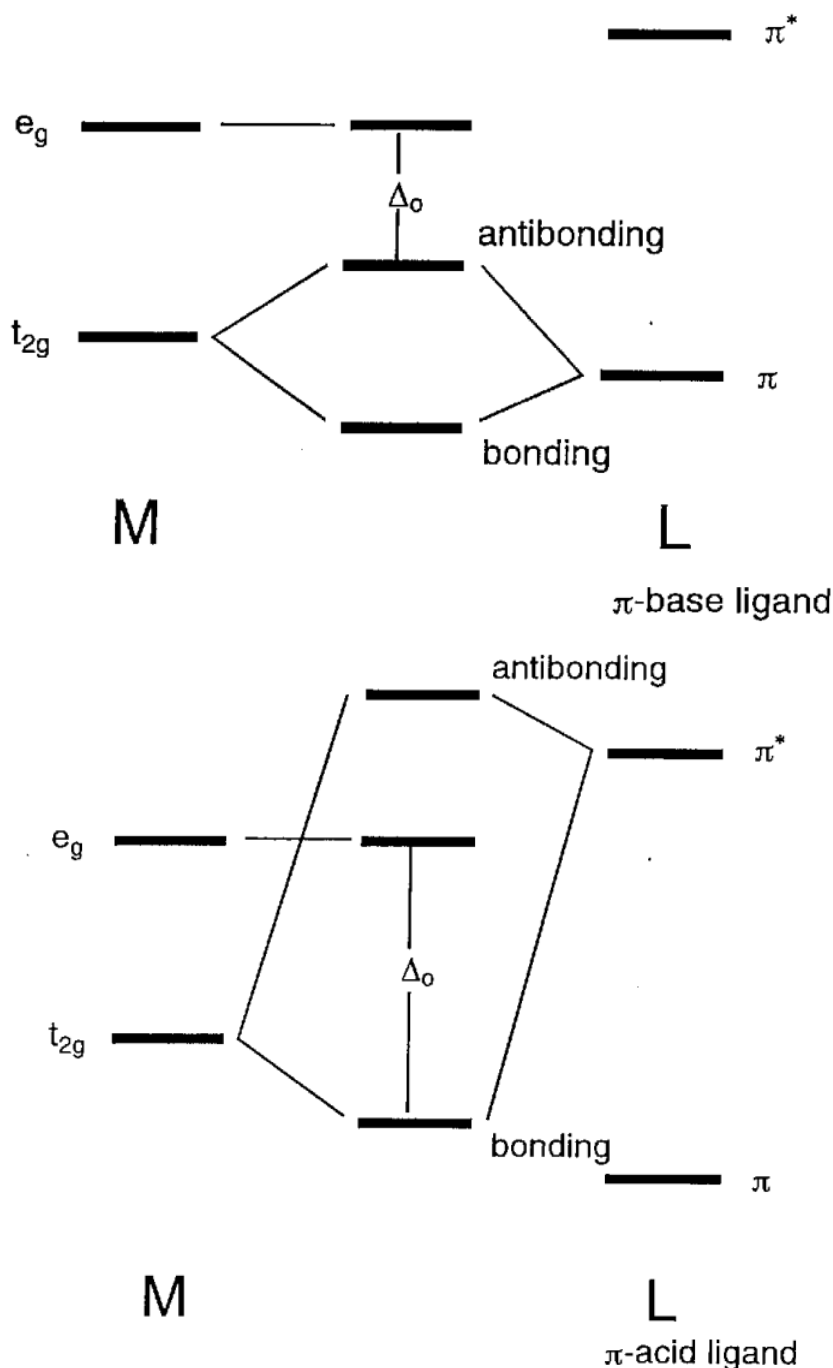


Figure 6.3.12: - The energy change upon formation of  $M-L_\pi$  bonds.

Using these simple molecular orbital considerations, the effects of  $\sigma$  and  $\pi$  orbital interactions between the metal and ligands upon the molecular orbitals are qualitatively understandable.

### Spectra

Many transition metal complexes have characteristic colors. This means that there is absorption in the visible part of the spectrum resulting from an electron being excited by visible light from a level occupied by an electron in a molecular orbital of the complex to an empty level. If the energy difference between the orbitals capable of transition is set to  $\Delta E$ , the absorption frequency  $\nu$  is given by  $\Delta E = h\nu$ . Electronic transitions by optical pumping are broadly classified into two groups. When both of the molecular orbitals between which a transition is possible have mainly metal d character, the transition is called a **d-d transition** or **ligand-field transition**, and absorption wavelength depends strongly on the ligand-field splitting. When one of the two orbitals has mainly metal character and the other has a large degree of ligand character, the transition is called a **charge-transfer transition**. Charge

transfer transitions are classified into metal (M) to ligand (L) charge-transfers (MLCT) and ligand to metal charge-transfers (LMCT).

Since the analysis of the spectra of octahedral complexes is comparatively easy, they have been studied in detail for many years. When a complex has only one d electron, the analysis is simple. For example, Ti in  $[\text{Ti}(\text{OH}_2)_6]^{3+}$  is a  $d^1$  ion, and an electron occupies the  $t_{2g}$  orbital produced by the octahedral ligand field splitting. The complex is purple as the result of having an absorption at 492 nm ( $20300\text{ cm}^{-1}$ ) (Figure 6.3.13) corresponding to the optical pumping of a d electron to the  $e_g$  orbital. However, in a complex with more than one d electrons, there are repellent interactions between the electrons, and the d-d transition spectrum has more than one absorptions. For example, a  $d^3$  complex  $[\text{Cr}(\text{NH}_3)_6]^{3+}$  shows two d-d absorptions in the 400 nm ( $25000\text{ cm}^{-1}$ ) region, suggesting that the complex has two groups of molecular orbitals between which an electronic transition is possible with a high degree of transition probability. This means that, when three electrons in the  $t_{2g}$  orbital are excited to the  $e_g$  orbital, there are two energy differences due to repellent interactions between the electrons.

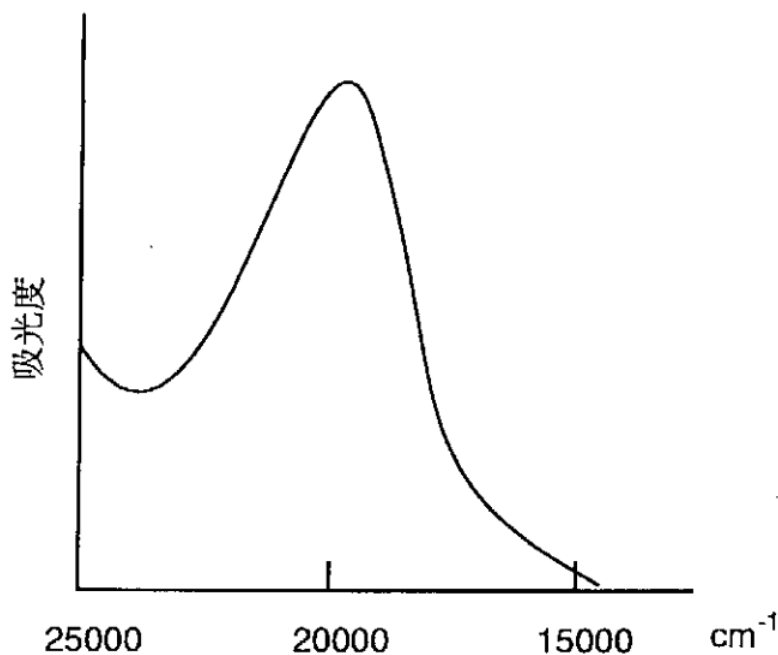


Figure 6.3.13: - A visible absorption spectrum of  $[\text{Ti}(\text{OH}_2)_6]^{3+}$ .

**Tanabe-Sugano diagrams** are constructed from calculations based on ligand field theory and have been widely used in the analysis of absorption spectra of  $d^1$  to  $d^9$  ions. The analysis becomes increasingly difficult for ions with many electrons. In any case, the existence of a d-d spectrum requires that the energy difference of an occupied orbital and an empty orbital is equivalent to the energy of the UV-visible spectrum, the transition is allowed by the selection rule, and the transition probability is high enough. Generally, a charge-transfer absorption is stronger than a ligand field absorption. An LMCT emerges when ligands have a non-bonding electron pair of comparatively high energy or the metal has empty low energy orbitals. On the other hand, an MLCT tends to appear when the ligands have low energy  $\pi^*$  orbitals, and bipyridine complexes are good examples of this. Since the lifetime of the excited state of a ruthenium complex  $[\text{Ru}(\text{bipy})_3]^{2+}$  is extraordinarily long, many studies have been performed on its photoredox reactions.

### Spectrochemical series

The magnitude of the ligand field splitting parameter  $\Delta_o$  is determined mainly by the identity of the ligands. An empirical rule called the **spectrochemical series** was proposed by a Japanese scientist Ryutarō Tsuchida. The rule was constructed from empirical data collected when spectra of complexes that have the same central metal, oxidation state, coordination number, etc. were measured. It is noteworthy that ligands with  $\pi$  acceptor properties are in a higher position in the series.



Although  $\Delta_o$  does become larger in this order, it is also dependent on the identity of the central metal and its oxidation state. Namely,  $\Delta_o$  is larger for 4d and 5d metals than for 3d metals and becomes larger as the oxidation number increases. The magnitude of  $\Delta_o$  is closely related to its absorption position in the electromagnetic spectrum, and is a key factor in determining the position of

a ligand in the spectrochemical series. A  $\pi$  donor ligand (halogen, aqua, etc.) makes the absorption wavelength longer, and a  $\pi$  acceptor ligand (carbonyl, olefin, etc.) shorter by contribution from the  $\pi$  bond.

## Magnetism

Magnetization,  $M$ , (magnetic dipole moment per unit volume) of a sample in a magnetic field,  $H$ , is proportional to magnitude of  $H$ , and the proportionality constant,  $\chi$ , depends on the sample.

$$M = \chi H$$

$\chi$  is the volume susceptibility and the product of  $\chi$  and the molar volume  $V_m$  of a sample is the **molar susceptibility**  $\chi_m$ . Namely,

$$\chi_m = \chi V_m$$

All substances have diamagnetism, and in addition to this, substances with unpaired electrons exhibit paramagnetism, the magnitude of which is about 100 times larger than that of diamagnetism. **Curie's law** shows that paramagnetism is inversely proportional to temperature.

$$\chi_m = A + \frac{C}{T}$$

where  $T$  is the absolute temperature and  $A$  and  $C$  are constants. In the Gouy or Faraday methods, magnetic moments are calculated from the change of weight of a sample suspended between magnets when a magnetic field is applied. In addition to these methods, the highly sensitive SQUID (superconducting quantum interference device) has been used recently to carry out such measurements.

Paramagnetism is induced by the permanent magnetic moment of an unpaired electron in a molecule and the molar susceptibility is proportional to the electron spin angular momentum. Paramagnetic complexes of d-block transition metals have unpaired electrons of spin quantum number  $1/2$ , and a half of the number of unpaired electrons is the total spin quantum number  $S$ . Therefore, the magnetic moment based only on spins can be derived theoretically.

$$\mu = 2\sqrt{2S(S+1)}\mu_B = \sqrt{n(n+2)}\mu_B$$

Here  $\mu_B = 9.274 \times 10^{-24} \text{ JT}^{-1}$  is a unit called the Bohr magneton.

Many 3d metal complexes show good agreement between the magnetic moments of paramagnetic complexes measured by a magnetic balance with the values calculated by the above formula. The relationship between the number of unpaired electrons and magnetic susceptibility of a complex is shown in Table 6.3.3. Because of this agreement with theory, it is possible to determine the number of unpaired electrons from experimental values of magnetic measurements. For example, it can be assumed that a  $\text{Fe}^{3+} \text{ d}^5$  complex with a magnetic moment of about  $1.7 \mu_B$  is a low-spin complex with an unpaired spin but a  $\text{Fe}^{3+} \text{ d}^5$  complex with a moment of about  $5.9 \mu_B$  is a high-spin complex with 5 unpaired electrons.

Table 6.3.3 Unpaired electrons and magnetic moments

Metal ion	Unpaired electron <b>n</b>	Spin-only magnetic moment ( $\frac{\mu}{\mu_B}$ )	
		Calculated	Measured
$\text{Ti}^{3+}$	1	1.73	1.7~1.8
$\text{V}^{3+}$	2	2.83	2.7~2.9
$\text{Cr}^{3+}$	3	3.87	3.8
$\text{Mn}^{3+}$	4	4.90	4.8~4.9
$\text{Fe}^{3+}$	5	5.92	5.9

However, the measured magnetic moment no longer agrees with the calculated spin-only value when the orbital angular momentum contribution to the magnetic moment becomes large. Especially in 5d metal complexes, this discrepancy between the measured and calculated values increases.

### ? Exercise 6.3.3

Calculate the spin-only magnetic moments of high spin and low spin  $\text{Fe}^{3+}$  complexes.

#### Answer

Since they are  $d^6$  complexes, a high spin complex has four unpaired electrons with the magnetic moment is  $4.90\mu_B$  and a low spin complex has no unpaired electron and is diamagnetic.

Some paramagnetic solid materials become **ferromagnetic** at low temperatures by forming **magnetic domains** in which thousands of electron spins are aligned parallel to each other. The temperature at which the paramagnetic-ferromagnetic phase transition occurs is called the **Curie temperature**. When spins are aligned antiparallel to each other, the material changes to an **antiferromagnetic substance**, and this transition temperature is called the **Néel temperature**. The material becomes ferrimagnetic when the spins are incompletely canceled. Recently, attempts have been made to synthesize polynuclear multi-spin complexes with special ligands that make paramagnetic metal ions align to induce ferromagnetic interactions between the spins. This effect is impossible in mononuclear complexes.

---

This page titled [6.3: Electronic Structure of Complexes \(Part 2\)](#) is shared under a [CC BY-NC-SA 3.0](#) license and was authored, remixed, and/or curated by [Taro Saito](#) via [source content](#) that was edited to the style and standards of the LibreTexts platform.